Chemical Reactivity and Electronical Properties of Graphene and Reduced Graphene Oxide on Different Substrates

E. Celasco[1,2,*]

[1]*Dipartimento di Fisica Università di Genova, Via Dodecaneso 33, 16146, Italy*
[2]*CNR IMEM Unità Operativa di Genova, Via Dodecaneso 33, 16146, Genova, Italy*

*Corresponding author: E-mail: celasco@fisica.unige.it; Tel: (+39) 010 353 6409

Received: 09 August 2018, Revised: 05 January 2019 and Accepted: 08 January 2019

DOI: 10.5185/amlett.2019.2204
www.vbripress.com/aml

Abstract

The chemical reactivity and the electronical properties variation of graphene (G) supported on Ni(111) and of the reduced Graphene Oxide (rGO) will be described thanks to the framework of University of Genoa and Polytechnic of Turin. We will present the main results obtained on the reactivity, towards CO, of pristine graphene grown on Ni(111). Single layer graphene films are grown by ethene dehydrogenation on Nickel, under different experimental conditions, and the system is studied *in-situ* by X-ray Photoemission and High-Resolution Electron Energy Loss Spectroscopies before and after CO exposure at 87 K and at room temperature.
The main results were:

- the best CO reactivity in the top-fcc configuration [**1**] of graphene on Ni(111), at low temperature [**2**]
- the higher reactivity occurs in the case of minimum percentage of contaminant or Ni_2C still present during the grown process.
- a reactivity toward CO at room temperature on graphene with punctual controlled defects by sputtering, with possible applications e.g., gas sensing [**3, 4**].

More applicative aspect is the modification of GO in rGO, by UV based process.
During the reduction, electrical properties is improved, opening possible application in the ink-jet printing mechanism as conductive printing system, coating or in the functionalization [**5**] of G.

Keywords: Graphene, graphene oxide, chemical reactivity, vibrational spectroscopy, surface chemistry.

Introduction

According to the exceptional properties of graphene (G), we would like to describe different approach of modification of this material in order to improve and optimize its chemical and electrical properties.

The first method consists in grown pristine graphene supported on strong interagent substrate as Nickel(111) [**1, 6**] with different growth parameter condition in order to optimized the CO reactivity at LT(87 K).

In order to obtain the same chemical reactivity also at room temperature, we found a method to induce punctual defects on graphene, founding a good reactivity at room temperature. To improve furthermore the electrical properties of this material, we studied a simple single step method of UV reduction of Graphene Oxide (GO) in polymeric matrix finalised to more applicative employment as ink-jet printing method.

The novelty of these two approaches consists in the following important experimental result: to find the reactivity toward CO on G/Ni(111), with punctual controlled defects, at room temperature, reducing the big limit of pristine G/Nickel system, which reactives only at low temperature (87K).

For the second method described we found a fast and low-cost procedure finalized to reduce GO at room temperature avoiding thermal treatments of other techniques.

The consequence of this approach consists in the possibility to extend the range of application of this reduction method on all the substrates which are not compatible with thermal treatments.

Experimental

The experiments of CO reactivity on supported graphene is perform ed in an ultra-high vacuum (UHV) chamber with base pressure $P = 2 \times 10^{10}$ mbar.

The spectroscopies employed are:

- high resolution electron loss (HREEL) spectrometer (Delta 0.5 by SPECS) HREEL spectra were recorded in-specular, with typical energy resolution is ~ 4.0 meV. The primary electron energy is Ee = 4.0 eV, and the angle of incidence of the

electron beam is ϑi = 62 (respect to the surface normal). The traces in all pictures were vertically shifted for sake of clarity.

- X-rays photoelectron spectroscopy (XPS) with a non-monochromatised X-ray source and hemispherical analyser (DAR 400 and EA125 by Omicron). The XPS spectra were recorded using Al-Kα excitation Photon at normal emission. The binding energy, E_b, has been calibrated on the metallic Ni 2p3/2 line located at 852.6 eV [**7**, **8**]. Other typical facilities for sample cleaning and residual gas analysis, a low energy electron diffractometer (LEED) and a four-degrees of freedom manipulator are present.

The sample can be heated to T > 1200 K by electron bombardment and cooled down to a temperature T = 87 K by fluxing liquid nitrogen. The nickel substrate Ni (111) a commercial single crystal disk of 10 mm diameter. Before each experiment, the Ni(111) crystal was cleaned by sputtering cycles with 3 keV Ne^+ ions followed by annealing to T = 1200 K. With XPS and LEED we can check every time the surface cleanliness and surface order. Single layer G films were grown *in-situ* by surface catalysed dehydrogenation of ethene, according optimized recipes by literature [**3, 9**].

The substrate growth temperature (Tg) was varied between Tg = 753 K and Tg = 873 K, for the different growth protocols obtaining different quality of pristine graphene and consequently different levels of CO reactivity at low temperature.

We will describe different protocols grown summarized in the following **Table 1**.

- 753 K Single dose (753 K SD) sample is referred to the procedure in which the substrate was exposed to ethene for 660 s at P = 5 x10^{-6} mbar (2500 L) keeping the substrate temperature at 753 K.
- 823 K Double dose 1 (823 K DD1) sample is obtained with a pressure P = 1.0 x 10^{-5} mbar (5000 L) for 660 s.
- 823 K Double dose 2 (823 K DD2) sample is obtained with the same conditions of DD1, but with a supplementary procedure finalized to optimizing the removal of C dissolved in the near-surface region. This procedure consists in exposing the samples to 2.5 L of O_2 at T = 673 K and then annealed to 783 K under UHV conditions during several cleaning cycles before the graphene growth.
- 873 K DD with a pressure P = 1.0 x 10^{-5} mbar (5000 L) for 660 s and the substrate temperature at 873 K.

The samples were kept eventually at Temperature growth (T_g) for 10 min after pumping ethane off.

Table 1. Different parameter for G/Ni growth.

Growth protocol	Temperature T_g (K)	Ethene dosing Pressure (mbar)	Growth time (s)	Ethene dose (l)	Waiting time thermalization without ethane gas (s)
753 K SD	753	5×10^{-6}	660	2500	600
823 K DD1	823	1×10^{-5}	660	5000	600
823 K DD2	823	1×10^{-5}	660	5000	600
873 K DD	873	1×10^{-5}	660	5000	600

CO exposure was performed by backfilling the chamber, after cooling the G/Ni(111) sample to 87 K or at room temperature (RT). In the case of GO a commercial reagent were used.

GO with thickness 0.7–1.2 nm was purchased from Cheap Tubes Inc. (USA) and it used without further purification.

The GO aqueous dispersions were deposited with spin-coating technique on the substrate after its cleaning procedure. The coated formulations were exposed with UV light for 2 min, (light intensity of 60 mW/cm^2). The samples were dried at 353 K under vacuum condition for 2 h, with the aim to remove the residual water. GOi in the following will indicate a printable GO/water dispersion formulated by mixing 0.02 g of GO powder in 4.5 g of deionized water. The lower concentration of GO was used to reduce the viscosity to a value compatible with the use of the inkjet nozzle. To additionally grind and disperse the GO agglomerates obtaining a homogeneous dispersion.

The employed conditions were: 30 min at 40 kHz with a additional 30 min at 59 kHz. In order to precipitate the larger and heavier particles on the bottom of the test tube is necessary one last step: the obtained dispersion was centrifugated at 14000 rpm for 5 min. The upper portion of this centrifuged dispersion was inserted into an ink reservoir, thus discarding the large precipitated particles. The resulting ink were tested at room temperature (RT) in a MicroFab Inkjet Printer with automatic 3D position control, using an 80 lm piezoelectric nozzle vibrating at a 250 Hz. The system printability of GOi formulation was evaluated on Silicon substrate.

Finally the formulations were prepared by adding 0.5 g of PEGDA and 0.08 g of PI to 4.5 g of distilled water in which 0.02 g of GO was previously dispersed (GO/PI ratio of 1/4 (GOp in the following).

Results and discussion

In the CO reactivity experiment, we monitored the relative CO reactivity, at low temperature (87 K) of different pristine obtained graphene. The most direct method is HREEL spectroscopy, with this method we have the possibility to investigate the specific energy loss, relative to the CO stretching, on the sample.

In **Fig. 1** panel a) are reported HREEL spectra of each preparations. The CO stretching region is around 256 meV. From the bottom to the top, in panel a), are reported spectra with increasing growth temperature: 753 K SD green spectrum, 823 K DD1 and DD2 pink and grey spectra respectively and 873 K blue spectrum.

The CO stretching mode, results weakly chemisorbed to the surface according to the flash temperature of desorption of 225 K as reported in more detail, in reference [**10**]. In panel a) it is evident a huge variability in reactivity finding the best condition with the growth temperature of 823 K. Also, the XPS spectra, of C1s region, reported in panel b) c) and d), of the same layout, presents different shapes, due to different weight

of graphene configurations. In more detail on the layout are represented the exact positions of single possible configuration of graphene respect to the Nickel substrate [**11**].

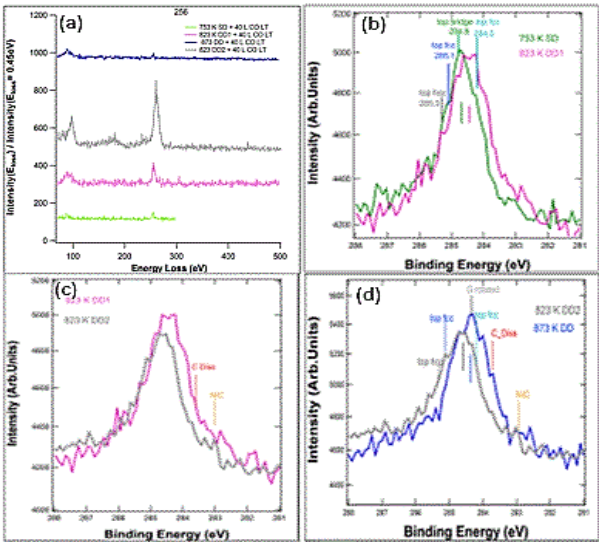

Fig. 1. Panel a) HREEL spectra on CO reactivity at LT of different pristine graphene growth parameters. Banel b) c) and d) comparison of XPS C1s shape of different preparations.

Starting from higher binding energy, we found top hcp, top fcc, top bridge and rotated graphene respect to the substrate, and the presence of nickel carbide or dissolved carbon [**11**]. In order to investigate in a more semi-quantitative way how these differences could influence the CO reactivity, an accurate fitting procedure was carried on reference Celasco *et al.*[2] One representative spectra of this fitting procedure is reported in **Fig. 2**, on 823 DD1 spectrum. The XPS peak was fitted with, six different components, according to the literature[11] described in more details in ref[2].

The position of the graphene respect to the substrate could be identified in

- Top fcc configuration. It presents a doublet at 284, 2 eV and 285, 1 eV of binding energy.
- Top bridge configuration at 284,8 eV
- Top hcp (not stable) at 285,3 eV
- Rotated graphene at 284,2 eV

We have also:

- Nickel Carbide at 283 eV
- Dissolved Carbon at 283,7 eV

We notice that the reactivity of single layer G on Ni(111) towards CO, a molecule depends on the relative position of the graphene domain with respect to the underlying substrate [**1, 12**] and on the amount of non graphenic carbon present in the surface layer. The reactive layer is graphene C atom sits in the fcc site. The confirmation of this aspect comes analysing the histogram of **Fig. 2b).**

The most reactivity film correspond to the one with higher amount of top fcc configuration (blue box in the histogram) and the minimization of NiC (red box) and dissolved carbon (orange box) that screening and reduce the reactivity. The hcp configuration (dark gray results not stable [**13**], while the top bridge (green box)is not active in the reactivity as rotated graphene component (gray) with screening action respect to the substrate.

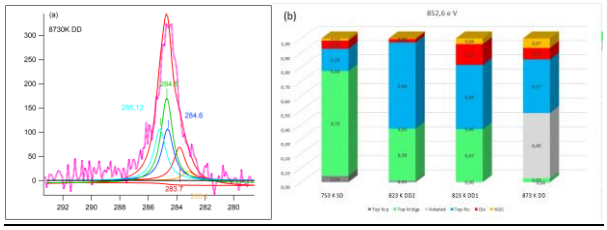

Fig. 2. Panel (a) example of XPS fitting of C1s peak. Panel (b) histogram of different Carbon configurations on each preparation film.

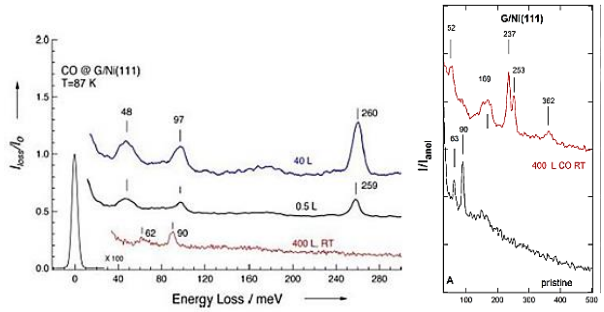

Fig. 3. Panel (a) HREEL spectra on CO dose at RT on pristine graphene (red spectrum) and LT CO dose on dark spectrum, 0, 5 L and blue spectrum, 40 L respectively. Panel (b) HREELS spectra on CO reactivity at RT on defected graphene film.

Another step of our experiments was the confirmation of the inertness activity of the pristine graphene on nickel at room temperature. A graphene film was grown with the optimized receipt and incremental dose of CO was done until the maximum one. In **Fig. 3** panel a) the pristine graphene layer was represented by the red line. After 400 L of CO no evidence of CO stretch is present. On the contrary at low T (87 K) even just 0.5 L of CO in sufficient to obtain a reactivity, 256 meV signal in the dark line. The saturation of CO stretch signal occurs after 40 L CO dose as described in the following. Different interesting behaviour occurs modifying the pristine graphene by sputtering. As reported in the HREEL spectra of **Fig. 3b** at room temperature in the red spectrum is evident the CO stretching vibration after 400 L CO dose.

The best sputtering conditions founded are:

I sample=1, 7 exp^{-7} A, E_{ion} 150 eV, for 1800 s.

In the same time a real time XPS cross check was done in order to avoid the ablation of graphene film during the sputtering dose[3]. With this method, we are able to have graphene on nickel reactive toward CO also at room temperature as evidenced in panel b) fo the following **Fig. 3**. In this panel the bottom dark spectrum corresponds to the pristine graphene film and the red spectrum correspond to the graphene film with induced punctual defects. It results reactive at room temperature according to the growth of the peaks at 237 meV and 253 eV after 400 L CO exposure. The first peak correspond to molecule – surface stretch mode and the second one to the internal C–O stretch mode for bridge

and atop configurations, respectively [**3, 14**]. In the panel b) of G*/Ni are presents three peaks related to the CO presence with an energy of the losses at 52 meV, 237 meV, and 253 meV respectively. They are close to those reported for CO/Ni(111) at high coverage (50 meV, 237 meV and 254 meV) [**14**]. The CO stretch frequency on G*/Ni is lower than the one reported for CO chemisorbed on pristine G/Ni at 90 K [**3, 10, 15**]. One possible conclusion is that CO reaches the Ni substrate through the vacancies.

The broad peak is visible at about 169 meV, (frequency close to the one of the D band in Raman spectra [**16**] it is considered a marker of surface disorder. The last loss at 362 meV present in panel b) corresponds to the C–H stretch resulting from water dissociation [**17**]. The induction of single controlled defects, open the possibility to have graphene supported on a strong interacting substrate as Nickel, reactive toward CO even if at room temperature.

In the second part of this paper we would like to describe a different modification of graphene-based material, studying more applicative aspects of the system graphene/graphene oxide.

In particular the possibility to be able to reduce GO in rGO or functionalize this system for different applications as ink jet printing [**6, 18**]. The method that we will describe, presents the advantage to start from a commercial, low cost material as graphene oxide reducing under UV light, as starting material. It results the most promising manufacturing technique that can be used to deposit polymers on a variety of substrates [**19**].

In the inkjet printing method, low viscosity should be maintained in the polymer precursor and it is necessary a fast polymerization occurs soon after the deposition. The UV curing process seems to be the best solution because it is performed at room temperature, allowing the ink polymerization even on thermal sensitive substrates such as paper, and in addition it is a fast-overall manufacturing process [**20**]. It presents the advantage of increase the range of possible applications respect to the process described in [**21**] with the thermal treatment.

A conductive printable ink, based on aqueous acrylic UV-curable formulations containing GO is used. The oxide presents the characteristics to be easily dispersed in water and it can be reduced during UV irradiation, in absence of thermal treatments. During this process we have the build-up of the crosslinking network. The polymer network acts as a binder during printing, decreases his resistivity of the acrylic polymer, during the *in situ* reduced GO, with the final result of a conductive percolative network.

In order to optimized the reduction, process the GO/PI weight ratio was varied from 1/0.25 to 1/8 (S1 = 1/0.25; S2 = 1/0.5; S3 = 1/1; S4 = 1/2; S5 = 1/4; S6 = 1/8 wt ratio). The UV reduction process to GO to rGO is monitored by XPS analyses and shown in details in [**22**]. The optimized results are reported in **Fig. 4** panel a) and b) with example of the variation of XPS C1s peaks after 2 min of UV irradiation of an aqueous dispersion containing 1 phr of GO and 4 phr of PI with respect to water.

In the panel a) and b) the fitting procedure on C1s peak acquired with XPS are reported. In both panels are present three contributions:

C-C, C=O and O-C=O bonds.

In order to monitor the occurrence of reduction from GO to rGO after UV, we will focus our attention on the middle peak related to C=O bond. In the panel b) it is evident a drastically reduction of this peak after UV treatment. This is a clear evidence of the reduction of the GO after UV.

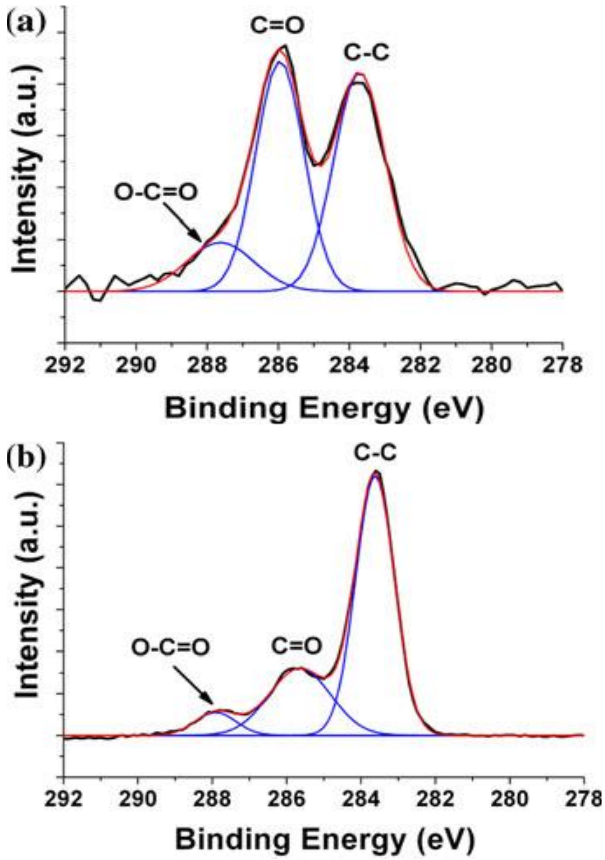

Fig. 4. Panel a) and b) XPS fitting on C1s peak before and after UV reduction on a ratio of GO/PI = ¼.

As final check of the reduction of resistivity an detailed electrical characterization was carried on and reported in **Fig. 5** panel a) and b). **Fig. 5** panel a) the test of this GO/ PEGDA/water ink by inkjet spotting straight line patterns set-up is reported. The test carried reported was performed with variable resolution (85–190 dots per- inch, dpi) and with a repetition from 1 to 5) of passes on the same track on microscope slides.

The reference sample for bulk nanocomposite material, is 100 lm thick films of the GOp, obtained by deposition on a microscope slide glass using a wire-wound bar. It was subsequently exposed to UV light for 2 min. The reference sample for electrical characterization, a PEGDA/PI thick film was similarly prepared without adding GO.

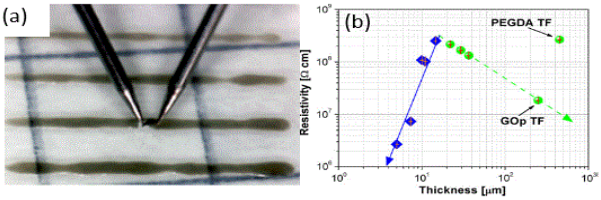

Fig. 5. Panel a two-point micro contact IV set up is reported while in panel b) Resistivity of GOp inkjet printed and thick film (TF) samples, as computed from linear fit to I–V curves, as a function of the sample thickness. The blue solid arrow is referred to the series of the inkjet printed tracks with single passes while the green dashed arrow to the multiple passes.

Fig. 5 panel b) shows the resistivity of thin printed layer samples as a function of sample thickness, compared to thick films of GOp (green arrow) and pure PEDGA (green dot). We observe a decrease of resistivity by over an order of magnitude (GOp TF versus PEGDA TF) after the addition of GO to PEGDA, after reduction by UV irradiation. For the printed samples, two trends may be evidenced, both concurring to a resistivity decrease.

Finally, by increasing the number of passes and thus the track thickness, a small decrease of resistivity is obtained (green dashed arrow in **Fig. 5**); this fact is normally due to an increased volume available for electrons' drift. Furthermore, reducing the dpi resolution by decreasing the amount of ink spotted on a single-pass track and consequently reducing the line thickness, a strong reduction of GO is obtained (as reported in the blue solid arrow in **Fig. 5**).

Those described samples show a decrease of resistivity, by two orders of magnitude with respect to the pure matrix. This behaviour may be explained considering that in a thin track a higher fraction of GO is reached and reduced by UV light than in a thick track, thus better contributing to electrical conduction [**22, 23**].

Conclusion

In this paper we compared different techniques of modification graphene-based material finalized to increase and tune the chemical and electronical properties. First results were increase graphene CO reactivities at low temperature (LT), varying the parameter graphene growth and the substrate cleaning in controlled manner. Following the optimization of the growth of pristine graphene, we try to induce punctual defect in order to obtain chemical reactivity toward CO also at room temperature.

Regarding the electrical properties, we optimized a UV reduction at room temperature of GO technique in order to obtain conductive polymer based on rGO. The more applicative aspect of this method is the employment of rGO in polymeric matrix in the ink jet technique.

The advantage of this second method described in the text, is the big range of application of this conductive polymeric matrix also on all the substrates not compatible with thermal treatments.

Acknowledgements

I would like to acknowledge:

- the UniGe Physics Dept. (Italy) head Staff M.A. Rocca and coworkers: G. Bracco, G. Carraro, A. Lusuan, J. Pal, L. Savio, M. Smerieri and L. Vattuone;
- the (DISAT) PoliTo (Italy) head staff G. Saracco, M. Sangermano and coworkers: M. Castellino, G. Cicero, D. Foix, F. Giorgis, A. Tagliaferro;
- the IIT@PoliTo (Italy) head staff C.F. Pirri and coworkers: K. Bejtka, A. Chiappone, A.Chiodoni, A. Chiolerio, R. Giardi, S. Porro, I. Roppolo.

This work was founded by PRA2013, FRA2016, FFABR 2018.

References

1. Dahal A.; Batzill, M.; *Nanoscale*, **2014**, *6*, 2548.
2. Celasco, E.; Carraro, G.; Smerieri, M.; Savio, L.; Rocca, M.; Vattuone, L.; *J. Chem. Phys.*, **2017**, *146.*
3. Celasco, E.; Carraro, G.; Lusuan, A.; Smerieri, M.; Pal, J.; Rocca, M.; Savio, L.; Vattuone, L.; *Phys. Chem. Chem. Phys.*, **2016**, *18*, 18692.
4. Schedin, F.; Geim, A. K.; Morozov, S. V.; Hill, E. W.; Blake, P.; Katsnelson, M. I.; Novoselov, K. S.; *Nat. Mater.*, **2007**, *6*, 652.
5. Roppolo, I.; Chiappone, A.; Bejtka, K.; Celasco, E.; Chiodoni, A.; Giorgis, F.; Sangermano, M.; Porro, S.; *Carbon N. Y.*, **2014**, *77*, 226.
6. Celasco, E.; in *Handbook of Graphene*, Eds. Mishra, S.; Patra, S.; Mishra, A.; WILEY-Scri, **2019**.
7. Biesinger, M. C.; Payne, B. P.; Lau, L. W. M.; Gerson, A.; Smart, R. S. C.; *Surf. Interface Anal.*, **2009**, *41*, 324.
8. Weatherup, R. S.; Bayer, B. C.; Blume, R.; Baehtz, C.; Kidambi, P. R.; Fouquet, M.; Wirth, C. T.; Schlögl, R.; Hofmann, S.; *ChemPhysChem*, **2012**, *13*, 2544.
9. Patera, L. L.; Africh, C.; Weatherup, R. S.; Blume, R.; Bhardwaj, S.; Castellarin-Cudia, C.; Knop-gericke, A.; Schloegl, R.; Comelli, G.; Hofmann, S.; Cepek, C.; *ACS Nano*, **2013**, *7*, 7901.
10. Smerieri, M.; Celasco, E.; Carraro, G.; Lusuan, A.; Pal, J.; Bracco, G.; Rocca, M.; Savio, L.; Vattuone, L.; *ChemCatChem*, **2015**, *7*, 2328.
11. Zhao, W.; Kozlov, S. M.; Höfert, O.; K. Gotterbarm, Lorenz, M. P. A.; Viñes, F.; Papp, C.; Görling, A.; Steinrück, H.P.; *J. Phys. Chem. Lett.*, **2011**, *2*, 759.
12. Weatherup, R. S.; Amara, H.; Blume, R.; Dlubak, B.; Bayer, B. C.; Diarra, M.; Bahri, M.; Cabrero-Vilatela, A.; Caneva, S.; Kidambi, P. R.; Martin, M. B.; Deranlot, C.; Seneor, P.; Schloegl, R.; Ducastelle, F.; Bichara, C.; Hofmann, S.; *J. Am. Chem. Soc.*, **2014**, *136*, 13698.
13. Zhao, W.; Kozlov, S. M.; Oliver, H.; Gotterbarm, K.; Lorenz, M. P. a.; Viñes, F.; Papp, C.; Andreas, G.; Steinrück, H.P.; *J. Chem. Phys. Lett.*, **2011**, *2*, 759.
14. Tang, S. L.; Lee, M. B.; Yang, Q. Y.; Beckerle, J. D.; Ceyer, S. T.; *J. Chem. Phys.*, **1986**, *84*, 1876.
15. Ambrosetti, A.; Silvestrelli, P.; *J. Chem. Phys.*, **2016**, *144*, 111101.
16. Ferrari, A. C.; Basko, D. M.; *Nat. Nanotechnol.*, **2013**, *8*, 235.
17. Politano, A.; Cattelan, M.; Boukhvalov, D. W.; Campi, D.; Cupolillo, A.; Agnoli, S.; Apostol, N. G.; Lacovig, P.; Lizzit, S.; Farias, D.; Chiarello, G.; Granozzi, G.; Larciprete, R.; *ACS Nano*, **2016**, acsnano.6b00554.
18. Giardi, R.; Porro, S.; Chiolerio, A.; Celasco, E.; Sangermano, M.; *J. Mater. Sci.*, **2013**, *48*, 1249.
19. Klauk, H.; *Nat. Mater.*, **2007**, *6*, 397.
20. Sangermano, M.; Bongiovanni, R.; Malucelli, G.; Priola, A.; *Nov. Sci. Publ. Inc., New York*, **2006**, *61*.
21. Sangermano, M.; Tagliaferro, A.; Foix, D.; Castellino, M.; Celasco, E.; *Macromol. Mater. Eng.*, **2014**, *299*, 757.
22. Novoselov, K. S.; Jiang, Z.; Zhang, Y.; Morozov, S. V.; Stormer, H. L.; Zeitler, U.; Maan, J. C.; Boebinger, G. S.; Kim, P.; Geim, A. K.; *Science*, **2007**, *315*, 1379.
23. He, H.; Klinowski, J.; Forster, M.; Lerf, A.; *Chem. Phys. Lett.*, **1998**, *287*, 53.

